Electrical Power and Energy Systems 125 (2021) 106474

Contents lists available at ScienceDirect

Electrical Power and Energy Systems

journal homepage: www.elsevier.com/locate/ijepes

Dynamic behaviour of a Francis turbine during voltage regulation in the electrical power system

E. Vagnoni[a,*], D. Valentin[b], F. Avellan[a]

[a] Laboratory for Hydraulic Machines, EPFL, Av. du Cour 33 bis, Lausanne 1004, Switzerland
[b] Center for Industrial Diagnostics and Fluid Dynamics, Polytechnic University of Catalonia (UPC), Av. Diagonal 647, ETSEIB, Barcelona 08028, Spain

ARTICLE INFO

Keywords:
Francis turbine
Synchronous condenser mode
Voltage regulation
Power stability
Full-scale prototype

ABSTRACT

Hydroelectric units can be operated in synchronous condenser mode to provide reactive power to the electrical power system (EPS) for voltage regulation. In this operating mode, the hydraulic turbine consumes active power and in case of hydroelectric units equipped with a Francis turbine, pressurized air is injected in the draft tube to decrease the tailwater level below the runner for decreasing the friction losses. Several dynamic phenomena have been recorded during full-scale hydraulic turbine operation due to the air–water mixing causing pressure and torque fluctuations which may compromise the operation and safety of both the hydraulic machine and the EPS.

In this paper, the study of the dynamic response of a Francis turbine prototype during synchronous condenser mode operation is performed to evaluate the transposition of the machine behaviour from the homologous reduced scale model to the full-scale prototype. Measurements of the pressure in draft tube cone, machine vibrations, and torque are performed in both full scale prototype and reduced scale model. The analysis of the dynamic behaviour of the hydraulic turbine focuses on the critical vibrations and power fluctuations. The onset of a sloshing wave in the draft tube cone is highlighted as predicted by the reduced scale model tests. Rotor–stator interactions (RSI) are analyzed and compared to the RSI during generating mode operation. The advantages of decreasing the pressure in the vaneless gap between the runner blades and the closed guide vanes by installing a draining pipe are emphasized to limit the amplitude of the fluctuations and to avoid unwanted two-phase flow phenomena in the vaneless gap which can perturb the machine operation and safety.

1. Introduction

The high Renewable Energy Sources (RES) scenario of the decarbonisation process [1] forecasts a 97% share of renewable electricity in the European power generation mix by 2050. The strong commitment on low carbon energy mix will require the massive integration of non-dispatchable RES and the disconnection and decommissioning of the so-called conventional units, namely the generating units of the fossil fuel thermal power plants. Moreover, several countries have the intention to further disconnect and decommission their nuclear power plants. The disconnection of these power plants and the penetration of intermittent renewable energies, such as wind and solar sources, in the power system cause the considerable increase of power fluctuations which must be compensated to guarantee the grid stability. Hydroelectric units are key players in the ambitious high RES scenario to support the electrical grid by balancing consumption and production for frequency regulation [2–5], and by providing reactive power for the voltage balance in the EPS by operating in synchronous condenser (SC) mode [6–9]. In this specific operating mode of the hydroelectric unit, Francis turbines are operated in dewatered condition to minimize the runner resistant torque and the corresponding power losses, while the electrical machine is providing reactive power to the EPS.

In SC mode, the guide vanes of the hydraulic machine are closed to block the incoming discharge and pressurized air is injected in the draft tube of the machine from a storage tank to maintain the tailwater level in the draft tube below the runner. Thus, the interference of the runner with water is minimized.

Few studies in literature investigated the behaviour of a hydraulic turbine during SC mode operation on a reduced scale physical model test-rig and highlighted complex air–water flow phenomena leading to dangerous vibrations. Tanaka et al. [10] described different two-phase flow phenomena observed in a reversible pump-turbine in SC mode. In his work, the sloshing motion of the water free-surface and other air–water interaction phenomena such as turbulent waves causing the

* Corresponding author.
E-mail addresses: elena.vagnoni@epfl.ch (E. Vagnoni), david.valentin@upc.edu (D. Valentin), francois.avellan@epfl.ch (F. Avellan).

https://doi.org/10.1016/j.ijepes.2020.106474
Received 24 May 2020; Received in revised form 6 August 2020; Accepted 24 August 2020
Available online 06 September 2020
0142-0615/

formation and entrainment of bubbles diffusing in the water volume and droplets interfering with the runner are observed. Vagnoni et al. [11–14] studied the SC mode operation of a reversible pump-turbine on a reduced scale physical model by investigating the air–water flow phenomena in both the draft tube cone and in the runner causing dangerous torque fluctuations, and the air losses in the machine. These studies highlighted the relevance of applying the densimetric Froude similitude to reach the similarity with the prototype. The densimetric Froude number is defined as:

$$Fr_d = \sqrt{\frac{\rho_{air}}{\rho_{water}}} \times \frac{\omega \times \sqrt{D}}{\sqrt{g}} \quad (1)$$

where ω is the angular speed of the runner (rad·s^{-1}), D (m) is the high pressure diameter of the Francis runner and g (m·s^{-2}) is the gravity. ρ_{air} and ρ_{water} (kg·m^{-3}) are the air and water density, respectively. The air density is computed from the ideal gas law by measuring the air static pressure in the cone of the draft tube and the temperature. It has been shown that the densimetric Froude number appears to be the most significant parameter in modeling the air–water interfaces [10,15–17].

These studies investigated the SC mode on a reduced scale model test and studied the scalability on a full size prototype but, in literature, there is a lack of published works about the evidence and validation of the behaviour of a full scale Francis turbine operating in synchronous condenser mode. Ceravola et al. [18] investigated the methodology for an efficient dewatering system at full-scale prototype and the influence of the water level on the sloshing wave. Valentin et al. [19] performed an experimental investigation on the effects of the transition to SC mode operation on the runner stresses and machine vibrations. In a recent patent presenting a novel hydraulic installation for SC mode operation, Guillaume et al. [20] evidenced the relevance of draining the water from the vaneless gap between the runner blades and the closed guide vanes by reducing the pressure in the spiral case to limit the power consumption and the machine vibrations. However, the draining of the vaneless gap is not always successful, especially in the case of units equipped by reversible Francis-type pump-turbines. In literature [7,10,12,13], it has been evidenced the formation of an air–water ring in the vaneless gap compromising the machine operation and safety in SC mode even by employing a draining pipe whose pressure reduction was not sufficient to fully drain the vaneless gap.

The present paper aims to investigate the dynamic behaviour of a Francis turbine prototype operating in synchronous condenser mode in comparison to the homologous reduced scale physical model. The goal is to evaluate the transposition of the machine behaviour in the reduced scale model to the dynamics in the full-scale prototype. Measurements of the active power, torque, runner stresses and guide vanes vibrations are performed on the full scale prototype to investigate the amplitude and the frequency of the fluctuations. A microphone close to the draft tube wall is used for investigating the sloshing motion. Measurement of the power and pressure fluctuations in several sections of the machine are performed on the homologous reduced scale model to study the flow dynamics and the machine vibrations by analogy with the full scale prototype. A previous study [11] investigated the sloshing motion and the torque response of the reduced scale physical model of the test case presented in this paper and it will be referred for comparison.

The experimental set-up in both the reduced scale model and in the full scale Francis turbine prototype operating in SC mode are described in Section 2. The results are presented in Section 3 with focus on the amplitude and frequency of the power and pressure fluctuations in both time and frequency domains. The results discussion follows in Section 4 for evaluation of the transposition of the machine dynamic behaviour observed in the reduced scale physical model and in the full scale prototype.

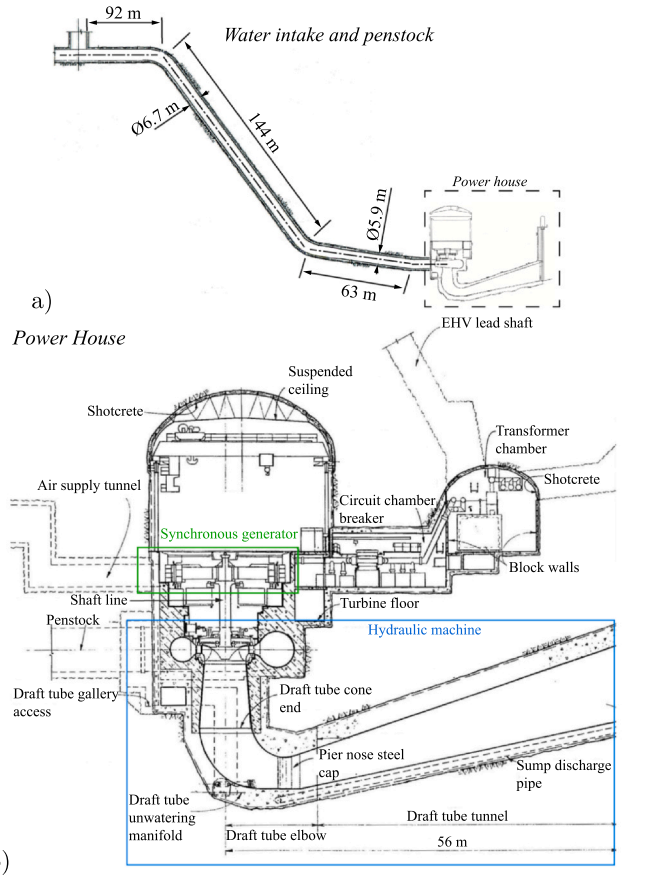

Fig. 1. Main dimensions of the penstock (a) and complete hydroelectric system (b).

2. Experimental set-up

2.1. Full scale prototype tests

Measurements are performed on a full-scale hydraulic unit featuring a synchronous electric machine and a Francis turbine with IEC specific speed $n_{ED} = 0.286$, defined as follows in Eq. (2), and featuring a runner with $D_P = 5.4$ m low pressure diameter, 16 blades and 20 guide vanes.

$$n_{ED} = \frac{D_P \times n}{E^{1/2}} \quad (2)$$

where n is the rotating frequency of the impeller s^{-1}, and E the machine specific energy. The turbine rated power, rotation speed and rated net head are $P_{rated} = 444$ MW, $N = 128.6$ min^{-1} and $H_{rated} = 170$ m, respectively. Main dimensions of the power plant penstock and the turbine prototype are illustrated in Fig. 1.

Tests are performed during synchronous condenser mode operation, at a runner rotational frequency $n_P = 2.14$ Hz and a gauge pressure $p_P = 1.2$ bar, which yield to compute $Fr_d = 0.55$. Pressurized air is injected in the draft tube cone to decrease the tailwater level at $0.7 \times D_P$ distance below the runner outlet. This value has been estimated by the regulation system of the air injection controlling the opening valve of the air admission system and the pressure in the air vessel. A water discharge flows through the runner labyrinth seal for cooling purpose, and a draining pipe, linking the vaneless gap between the closed guide vanes and the draft tube cone, is installed to evacuate the cooling discharge from the runner chamber, as illustrated in Fig. 2. Furthermore, tests are also performed in generating mode, which means that the hydraulic machine is fully submerged in water and the transmitted torque at the runner shaft is positive, i.e. active power is produced. The

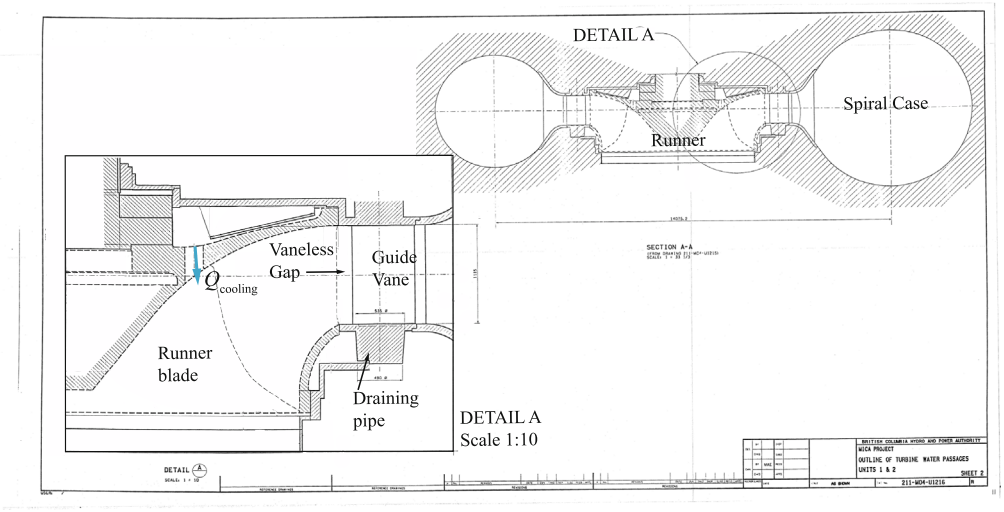

Fig. 2. Scheme of the turbine water passages of the full-scale prototype configuration during SC mode operation.

Table 1
Operating conditions at which measurements are performed on the full scale prototype.

Operating Mode:	N_{ED} (–)	Q_{ED} (–)	P (MW)
Synchronous condenser mode	0.286	–	−12
Generating mode	0.286	0.20	400

operating condition at generating mode is set at IEC discharge coefficient $Q_{\mathrm{ED}} = \frac{Q}{D_P^2 \times E^{1/2}} = 0.20$ and $P = 400$ MW, for comparison to the machine behaviour during the SC mode operation, as illustrated in Table 1. The apparent power, active power and reactive power during both SC mode and generating mode are presented in Fig. 3. It can be observed that in generating mode, the apparent power coincides with the active power produced by the machine, and there is no supply of reactive power. In SC mode, the active power consumed by the machine is lower than the apparent power and reactive power is supplied to the power system for voltage support.

On-site measurements of the runner stresses and of the torque are performed by employing on-board strain gauges on the runner blade and on the runner shaft, respectively. The dynamic pressure is measured by installing a tap wall pressure sensor in the draft tube cone at $0.4 \times D_P$ distance below the runner outlet. Vibrations of the machine are also recorded by using an accelerometer (Kistler 8752A, 100 mV/g) in the guide vanes and a microphone on the draft tube wall. The complete list of sensors installed during the tests is presented in [21]. All the signals were simultaneously acquired with a B&K LAN XI module (Pulse module) and all measurements have been recorded at a sample frequency $f_{\mathrm{samp}} = 4096$ Hz.

2.2. Reduced scale physical model tests

The homologous reduced scale physical model of the turbine prototype described in Section 2.1 features a runner with $D_M = 0.35$ m low pressure diameter and is installed in a closed-loop test rig, as illustrated in Fig. 4 and fully described in [22]. The guide vanes are closed and a system of air injection is installed in the draft tube cone to decrease the water level at $0.7 \times D_M$ downstream the runner outlet which corresponds to the setting of the water level in the full scale prototype. The gauge pressure is set constant at 1.2 bar, and the rotational frequency of the runner at $n_M = 11.3$ Hz to fulfill the densimetric Froude similarity with the prototype. Water is injected through the labyrinth seal for cooling purpose. Differently from the full-size prototype, the reduced scale physical model does not include a draining pipe.

Wall pressure measurements are performed in several sections of the machine at the inlet pipe, spiral case, and draft tube as illustrated in Fig. 5. The positions of all sensors with respect to the turbine frame of references are listed in Table 2. The dynamic pressure is measured by flush-mounted piezo-resistive pressure sensors. They allow for pressure measurements in the range of 0–5 bar with a maximum mum measurement uncertainty of 0.7%. The sample frequency is set at 3000 Hz.

3. Results

3.1. Sloshing motion detection

To investigate the sloshing motion frequency in the full scale prototype of the Francis turbine, the analysis of both the pressure and the wall vibrations in the draft tube cone is conducted. In particular, the Discrete Fourier Transform (DFT) is applied to the pressure sensors and microphone signals to highlight the dominant frequency in the draft

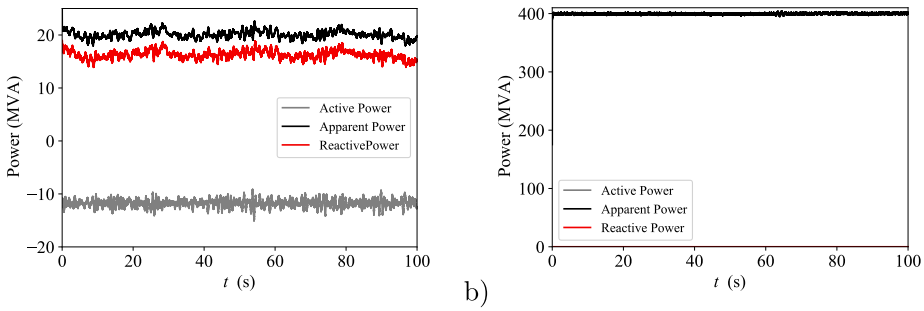

Fig. 3. Time-history of the Active Power, Apparent Power and Reactive Power during SC mode (a) and generating mode (b).

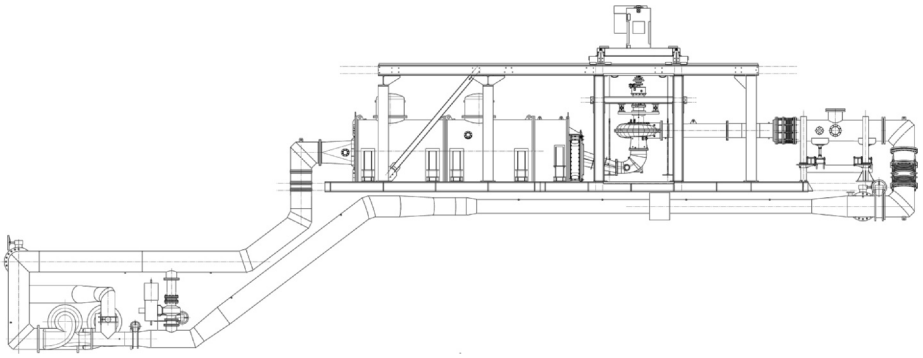

Fig. 4. EPFL closed-loop test rig, featuring two axial pumps and complying with the IEC60153 standard for reduced scale physical turbine model tests (I. E. Commission, et al., Hydraulic turbines, storage pumps and pump-turbines – model acceptance tests, Standard No. IEC 60193, International Electrotechnical Commission, 1999).

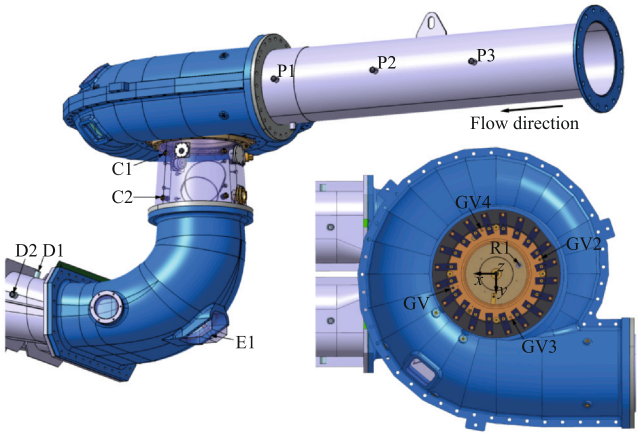

Fig. 5. 3D view of the reduced scale model of the investigated Francis turbine.

Table 2
Tap wall pressure sensors position in respect to the runner horizontal and vertical axis.

Sensor #	Sensor	Description	z [mm]	x [mm]	y [mm]
1	P1	Upstream pipe	0	−787	701
2	P2	Upstream pipe	0	−1365	702
3	P3	Upstream pipe	0	−1943	702
4	GV1	Guide Vanes	36	220	71.5
5	GV2	Guide Vanes	36	- 220	−71.5
6	GV3	Guide Vanes	36	−71.5	220
7	GV4	Guide Vanes	36	71.5	−220
8	R1	Runner	−78	−120.5	−46.3
9	C1	Cone Upper Section	−237	91.5	159
10	C2	Cone Lower Section	−477	100	174
11	E1	Elbow	−1105	0	0
12	D1	Diffuser	−853	846	237
13	D2	Diffuser	−969	877	415

tube cone.

The Froude number of the sloshing free-surface is introduced as a function of the measured frequency f_{sloshing} and of the wave length πD of the sloshing motion as follows:

$$Fr_{\text{sloshing}} = \frac{f_{\text{sloshing}} \times \pi D}{\sqrt{g \times \pi D}} \tag{3}$$

where D is the diameter of the section the draft tube cone where the tailwater level is located in steady state. This non-dimensional number allows for the comparison of the sloshing wave frequency values for different water volumes and different operating conditions, as detailed in [11] and it will be employed for comparison and validation of the predicted value of the sloshing frequency by the reduced scale model tests.

The time-history and the DFT of the draft tube wall vibrations are presented in Fig. 6. The spectrum of the wall vibrations in the draft tube cone evidences a pressure peak which is specific of the synchronous condenser mode operation at $f_{\text{sloshing}} = 0.55$ Hz. In generating mode, as presented in Fig. 6b), the spectrum of the wall vibrations does not exhibit this oscillation, indeed, this fluctuation likely represents the sloshing wave.

The time-history of the pressure coefficient in the draft tube cone is presented in Fig. 7. The pressure coefficient c_p is calculated as follows in Eq. (4).

$$C_p = \frac{p(t) - \bar{p}}{\rho E} \tag{4}$$

where ρ is the water density, $p(t)$ is the instantaneous pressure measured by the pressure sensor in the draft tube cone and $\bar{p}$ is the mean value of $p(t)$ over the measurements acquisition period. As illustrated in Fig. 7, the DFT of the pressure in the draft tube cone shows that the dominant peak is at a frequency lower than 0.1 Hz which is due to the variation of the downstream water level, while there is a lack of significant peak amplitude corresponding to the sloshing frequency. It suggests that the sloshing motion cannot be detected by employing this pressure sensor in the draft tube cone. The sensor is located in air,not in water, and, the oscillation of the pressure in the air volume can be up to

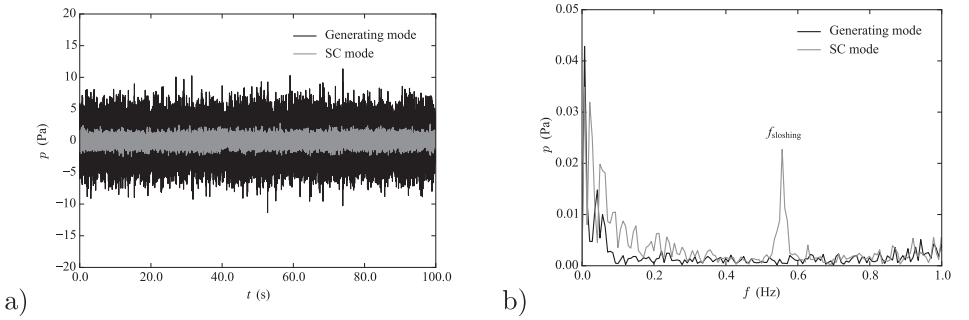

Fig. 6. Time-history (a) and spectrum (b) of the draft tube wall vibrations of the full scale prototype operating in SC mode and in generating mode.

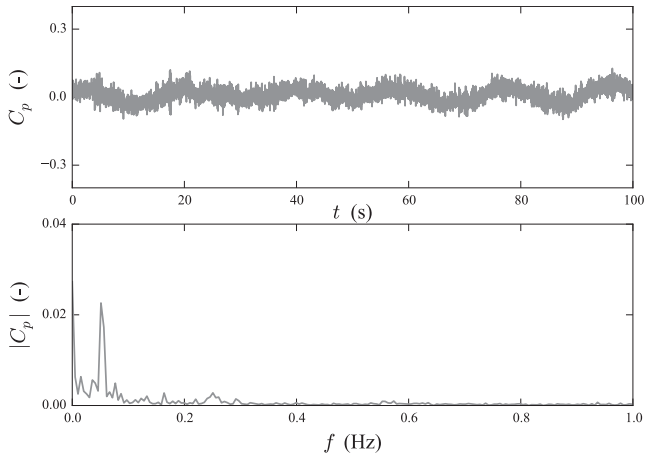

Fig. 7. Time-history and spectrum of the pressure coefficient of the draft tube cone of the full scale prototype operating in SC mode.

10^2 times lower in magnitude than the oscillation in water and, therefore, hard to distinguish within the spectrum in frequency domain, as also observed in the reduced scale model.

3.2. Runner and guide vanes vibrations on the full scale prototype

The time-history and the spectrum of both runner stresses and guide vanes vibrations signals in the full scale prototype are presented in Fig. 8. The root mean square (RMS) of the vibrations and stresses signals are computed as follows in Eq. (5) to evaluate the fluctuations amplitude.

$$\mathrm{RMS} = \sqrt{\frac{1}{n_s}\sum_{k=1}^{n_s}(C_k - \overline{C})^2} \tag{5}$$

where C_k is the instantaneous signal of vibrations or stresses, $\overline{C}$ the mean value of the signal, and n_s the number of samples. It is observed that the amplitude of both runner blades stresses and guide vanes vibrations are considerable in generating mode, while they decreases in SC mode. The RMS value of the runner blades stresses in SC mode is RMS = $3E^{-6}$ m/m which is 80% lower than the RMS value in generating mode. Similarly, the guide vanes at the BEP in generating mode experiences vibrations with RMS = 2 ms^{-2} while they have a limited amplitude in SC mode with a RMS value RMS = 0.2 ms^{-2}. By computing the DFT of the signals, presented in Fig. 9, the dominant frequency of the stresses in the rotating components of the machine (runner blades) is f_s = 42.66 Hz which corresponds to the guide vanes passing frequency in the rotating frame in both SC mode and generating mode. As shown in Fig. 9b), it appears that the dominant frequency of the vibrations of the stationary part of the machine (guide vanes) in SC mode is proportional to the blade passing frequency f_b = 34.36 Hz, which also corresponds to the dominant frequency in the stationary part of the machine in generating mode. Both dominant oscillations result from the rotor–stator interaction phenomenon due to the combination of the pressure fields of the rotating part and the one of the stationary part of the machine [23].

The time-history and spectrum of the torque T at the runner shaft are presented in Fig. 10 in SC mode and generating mode. Both the operating modes feature a torque oscillation signal with RMS = $4E^{-12}$ m/ m. The frequency of this dominant fluctuation corresponds to the natural frequency of the torsional mode of the shaft. Therefore, the torque at the runner shaft exhibits no significant perturbations.

As also observed in the reduced scale model tests [11], the sloshing motion does not disturb the machine operation since the measurements of both torque and runner stresses show no fluctuation at the frequency of the sloshing motion or close to this frequency value.

In Fig. 11, the time-history and the spectrum of the power consumed by the machine during the SC mode operation is presented and compared to the active power produced in generating mode. Clearly, the reduction of the tailwater level below the runner allows for reducing the consumption of the active power to the 3% of the rated power. Furthermore, during the SC mode operation, it is measured RMS = 0.77 MW, which is slightly higher than the RMS value in generating mode RMS = 0.64 MW. However, both values evidence that the machine operation is not perturbed.

3.3. Runner and guide vanes vibrations on the reduced scale physical model

The measurement of the pressure fluctuations in the sections of the reduced scale model listed in Table 2 are studied to investigate the formation of two-phase flow phenomena perturbing the machine operation during the SC mode operation. In particular, the RMS of the pressure coefficient is computed as in Eq. (5) to evaluate the pressure fluctuations amplitude in all sections of the machine. As it can be observed in Fig. 12, the highest RMS values are experienced by the guide vanes of the turbines. The cooling water discharge and the water in the draft tube entrained by the runner blades form an air–water flow in the vaneless gap between the closed guide vanes and the runner blades. As a draining pipe is not installed in the reduced scale model set-up, this flow cannot be evacuated from the runner chamber and it is pushed against the closed guide vanes due to the centrifugal force given by the rotating blades of the runner. This phenomenon, so called air–water ring, has been already observed in [13] and it has been demonstrated being the cause of important machine vibrations and power swings during the SC mode operation.

In Fig. 13a), the time-history and the spectrum of the pressure fluctuations in the guides vanes, position GV2, are presented. As highlighted in the spectrum of the pressure measured in the guide vanes, a clear fluctuation is identified at a frequency value corresponding to the runner rotational frequency and to its harmonics. There is a disagreement with the measurement of the guide vanes vibrations

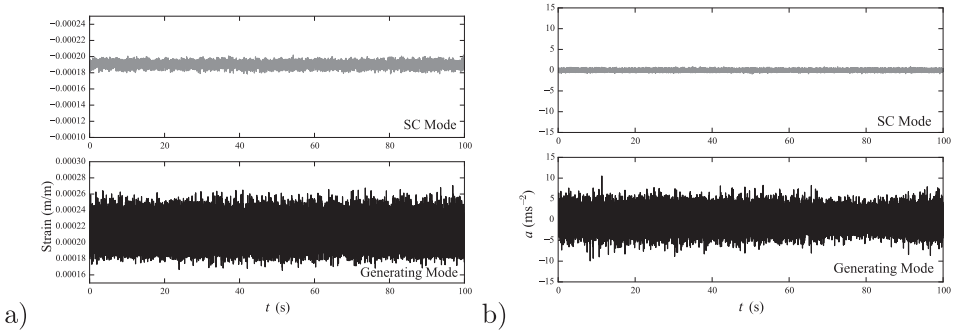

Fig. 8. Time-history of the measurements of the stresses at the runner blades (a), guides vanes vibrations (b) of the full scale prototype operating in SC mode and generating mode.

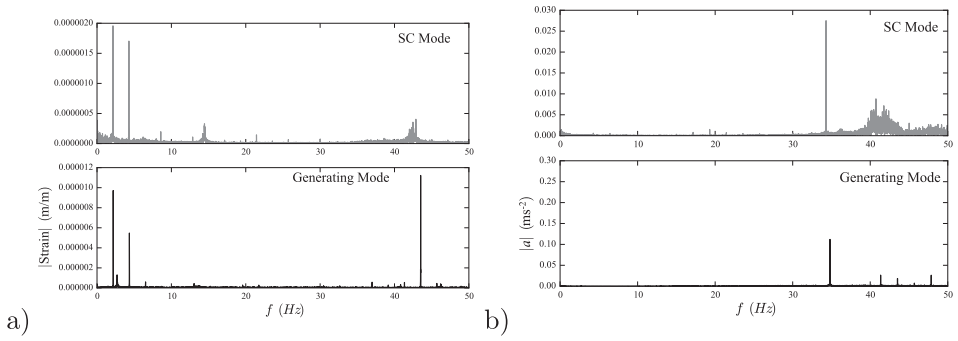

Fig. 9. Spectra of the runner blades stresses (a), and of the guides vanes vibrations (b) of the full scale prototype operating in SC mode and in generating mode.

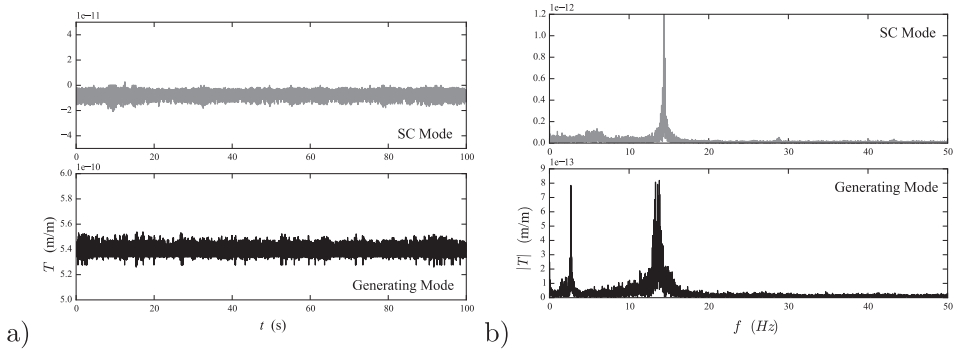

Fig. 10. Time-history (a) and spectrum (b) of the torque at the runner shaft of the full scale prototype operating in SC mode and in generating mode.

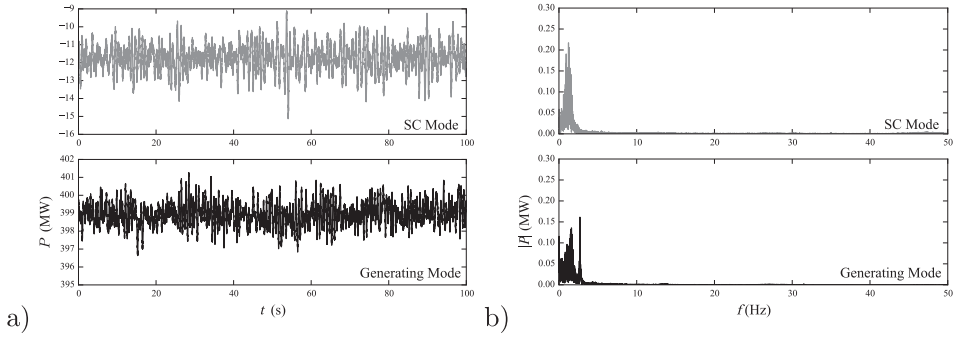

Fig. 11. Time-history (a) and spectrum (b) of the active power consumed by the full scale prototype operating in SC mode and in generating mode.

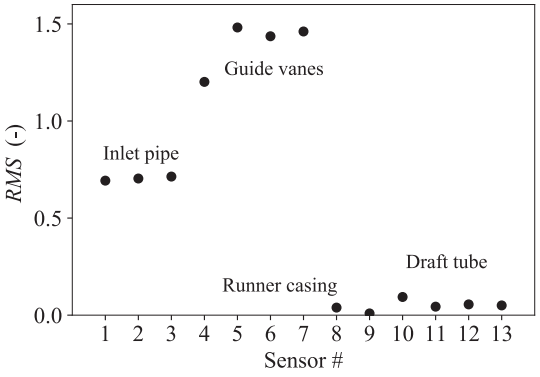

Fig. 12. RMS of the pressure coefficient in all measurement sections of the reduced scale model during SC mode operation.

in the full scale prototype which, instead, presents a dominant peak at the blade passing frequency. Furthermore, by observing the time-history of the signal, a periodic drop of the pressure fluctuation is observed at a very low frequency f_P = 0.3 Hz. By comparing this signal with the time-history of the pressure fluctuations in the upstream pipe, location P1, also illustrated in Fig. 13a), the pressure fluctuations at P1 decrease, and the recurrent drop of the pressure coefficient is not observed. In Fig. 13c), the auto-spectrum of the pressure measured in P1 is illustrated for comparison with the spectrum of the pressure measured in the guide vanes of the machine. By computing the cross-correlation and the coherence between these two pressure signals, the correlation of the fluctuations of the two signals is highlighted, as presented in Fig. 14. It is noted that the coherence of the two signals is higher than 90% at the frequency value equal to the angular frequency of the runner and its harmonics.

In Fig. 15, both time-history and spectrum of the consumed active power are illustrated. The evidence of the low-frequency fluctuation f_P = 0.3 Hz, observed also in the pressure pulsation in the guide vanes, is highlighted. This provides a further confirmation of the presence of a dominant pulsation during the SC mode which is linked to the formation of the air–water ring in the vaneless gap between the closed guide vanes and the runner blades.

The coherence and cross-correlation between the measurements of the active power and the pressure fluctuation in both the guide vanes and in the upstream pipe are illustrated in Fig. 16a), respectively. The

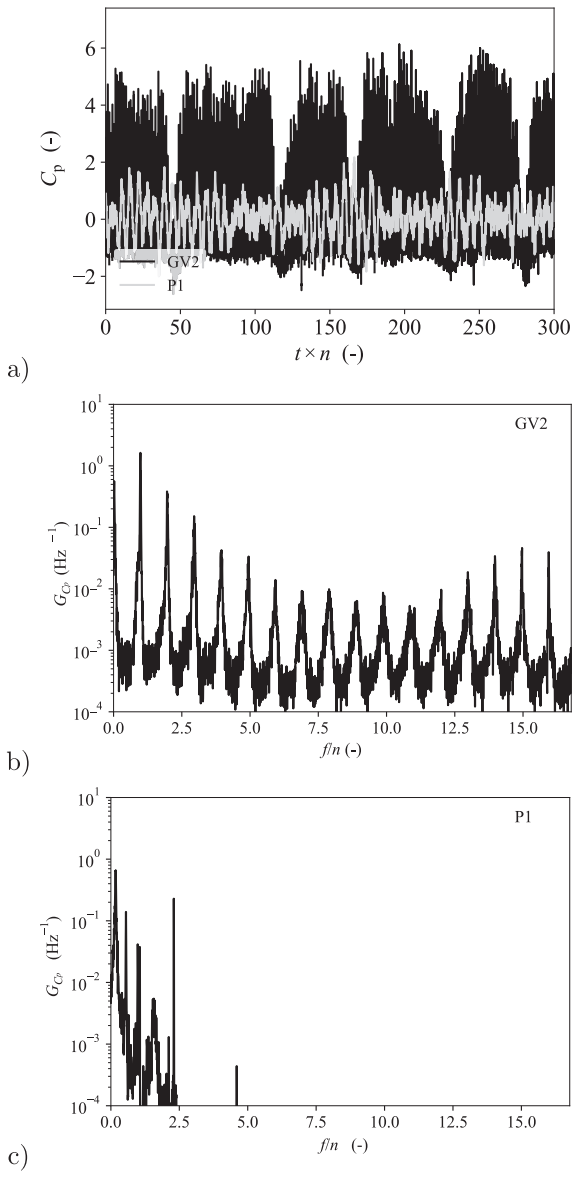

Fig. 13. Time-history (a), and auto-spectrum (b) of the pressure fluctuations in the guide vanes and in the inlet pipe in the reduced scale model during SC mode operation.

correlation of the oscillation of the active power and the pressure in the guide vanes is here highlighted at $f_P = 0.3$ Hz. It is also noticed that this fluctuation is not recorded in the upstream pipe, since the coherence with the power signal is higher than 80% only for a frequency value synchronous to the rotational speed of the runner. As illustrated in Fig. 15 and Fig. 16, the presence of an air–water ring in the vaneless gap causes strong power and pressure fluctuations in the machine at a frequency lower than the blade passing frequency which may lead to dangerous vibrations and power swings.

4. Discussion

4.1. Sloshing motion dynamics transposition

The investigation of the sloshing motion on the reduced scale physical model of the Francis turbine studied in this paper, has been previously conducted by Vagnoni et. al. [11]. This study highlighted that the dominant frequency of the sloshing motion corresponds to the free-surface gravity wave natural frequency f_{wave} plus a correction which varies between 10% and 15% of f_{wave} depending on the densimetric Froude number:

$$f_{sloshing} = f_{wave} + \delta f\,(Fr_d) \tag{6}$$

where $f_{wave} = \frac{1}{2\pi}\sqrt{\frac{1.84g}{D/2}}$ for a cylindrical container of diameter D. For $Fr_d = 0.55$, the reduced scale model predicts $\delta f = 0.12 \cdot f_{wave}$.

In the case of the full scale prototype, the above expression yields to $f_{sloshing} = 0.45$ Hz with $f_{wave} = 0.4$ Hz by considering that the free-surface is located at $0.7 \times D_P$ downstream the runner outlet. If compared to the this value, the sloshing frequency measured in the prototype $f_{sloshing} = 0.55$ Hz, as presented in Section 3.1, is 10^{-1} Hz higher than the value predicted by the study of the sloshing motion in the reduced scale model tests. By comparing the Froude number of the sloshing free surface in the full size prototype with the results achieved in [11], it is noticed that a fairly good agreement is achieved by considering an RMS value on the frequency measurement RMS = 0.025 Hz, as highlighted in Fig. 17. The correspondence of the Froude number of the sloshing free surface further confirms the validity of the performed study and theoretical framework on the sloshing prediction by the reduced scale model tests.

4.2. Importance of the draining pipe

As observed in Section 3.2, the amplitude of the runner and guide vanes vibrations significantly decreases during the SC mode operation in the full scale prototype in respect to the oscillation amplitude in generating mode.

The decrease of the amplitude of the oscillations on the full scale prototype suggests that the runner is completely drained in SC mode thanks to the compressed air injected into the draft tube cone, and to the draining pipe which plays a key role in draining the water from the vaneless gap between the runner blades and the guide vanes. The draining pipe system decreases the pressure in the vaneless gap, by allowing the water to completely flow out the runner chamber.

Therefore, in the Francis turbine prototype studied in this paper, there is no evidence of the air–water ring due to the low amplitude of

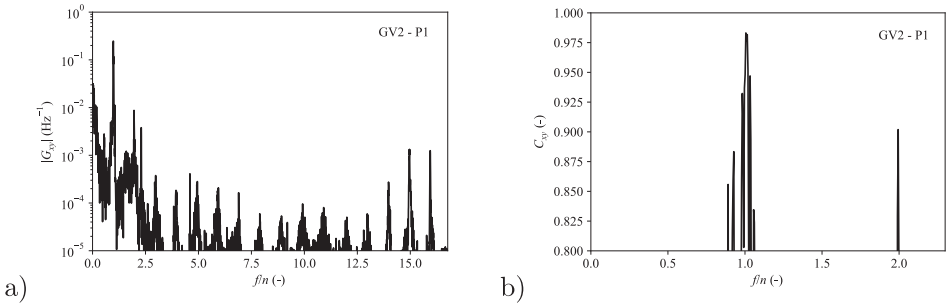

Fig. 14. Cross-correlation (a), and coherence (b) between the measurement of the pressure fluctuation in the guide vanes and in the inlet pipe in the reduced scale model during SC mode operation.

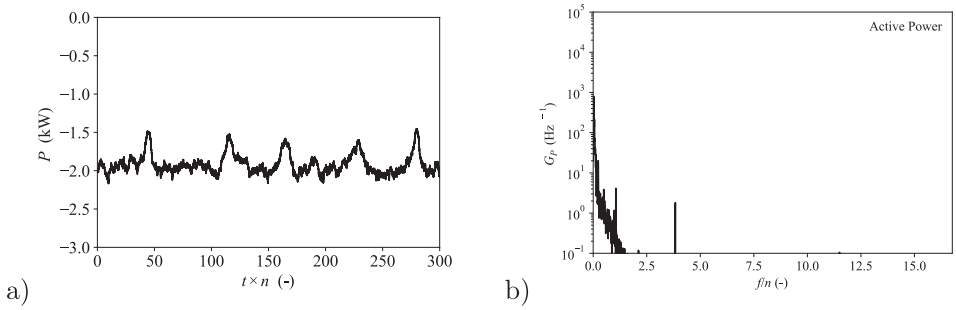

Fig. 15. Time-history (a) and auto-spectrum (b) of the active power at the reduced scale model runner shaft in SC mode.

vibrations in the runner and guide vanes, and to the rotor–stator interaction happening at the same frequency than in generating mode. It has been shown that the value of the RSI dominant frequency decreases in SC mode in respect to the dominant frequency in generating mode due to the presence of the air–water ring in the vaneless gap [12].

Furthermore, the analysis on the torque and the active power measurements does not evidence perturbations in the machine operations which further confirms the complete drain of the runner avoiding the formation of two-phase flow phenomena interacting with the runner.

The consequences of a lack of the draining pipe in the machine set-up during SC mode operation is highlighted in the results achieved by the reduced scale model tests. As presented in Section 3.3, strong power and pressure fluctuations at a frequency lower than the blade passing frequency are recorded in the machine, and these oscillations can lead to dangerous vibrations and power swings. Therefore, when the draining pipe is not installed and the runner chamber is not drained, the water droplets coming from the sloshing wave in the draft tube cone and entrained by the runner blades, and the cooling water discharge coming from the runner labyrinth seal can accumulate in the vaneless gap and dramatically raise the power consumption and both power and pressure fluctuations by extending the risk of damaging the mechanical and electrical system.

The draining pipe, assuring the draining of the runner chamber, is proved to be fundamental for a safe operation of a Francis turbine during the SC mode of the hydroelectric unit for the voltage regulation of the EPS. Furthermore, to reproduce the machine behaviour of the full scale prototype in SC mode on the homologous reduced scale model, the installation of the draining pipe should be required.

4.3. Transposition of the power consumption

The differences in the dynamic behaviour of the machine at full scale and at reduced scale, because of the draining pipe on the full scale prototype, highlight the benefits of having a completely drained vaneless gap which guarantees the reduction of vibrations which may lead to the increase of the power consumption. On the other side, a complete validation of the transposition of the results achieved on the reduced

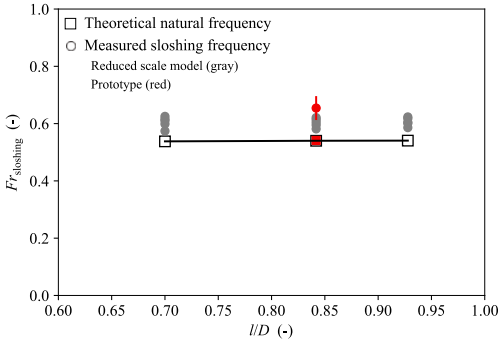

Fig. 17. Froude number of the sloshing free surface as a function of the water level l divided by the inner diameter of the cone D for the investigated Fr_d values in the reduced scale physical model (gray) for different water levels and densimetric Froude number [11] and in the full-scale prototype (red). (For interpretation of the references to colour in this figure legend, the reader is referred to the web version of this article.)

scale model to the full scale prototype cannot be fulfilled. However, the analysis on the power consumption in both the full scale prototype and the reduced scale model tests suggests a possible transposition of the results by computing P_{nD}, the IEC power coefficient, as follows:

$$P_{nD} = \frac{P}{\rho n^3 D^5} \tag{7}$$

While the water density is considered for a Francis turbine operating in generating mode, in SC mode, the air density should be considered instead due to the influence of the pressure on the fluid surrounding the runner. In Fig. 18, the comparison between the time-history of P_{nD} of the full scale prototype and of the reduced scale model is presented for the SC mode operation. This comparison shows that the absolute mean value $\overline{P}_{nD}$ is higher in the reduced scale model than in the prototype, being $\overline{P}_{nD} = -270$ in the reduced scale model and $\overline{P}_{nD} = -193$ in the full scale prototype. Furthermore, the RMS and the peak values evidence a significant fluctuation on the reduced scale model which is not observed in the prototype. It is noticed that the maximum value of P_{nD} in

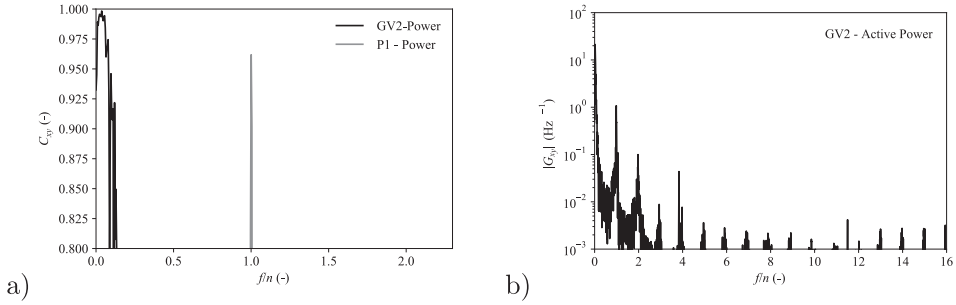

Fig. 16. Coherence (a) and Cross-spectrum (b) between the torque and the pressure fluctuation measurement in GV2 in the reduced scale model during SC mode operation.

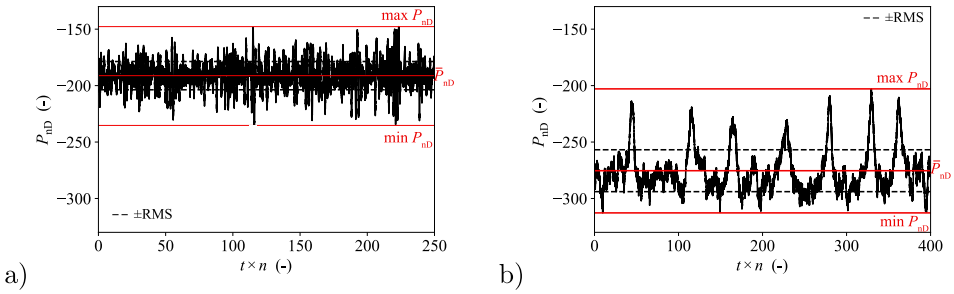

Fig. 18. Time-history of the IEC power coefficient during synchronous condenser mode operation in both full scale prototype (a) and reduced scale model (b) of the studied Francis turbine.

the reduced scale model, corresponding to the peak value of the oscillation, is $P_{nD,max} = -201$, value which is close to $\overline{P}_{nD}$ in the full scale prototype by taking into account also the RMS value RMS = 11. This can be explained by considering a pulsation of the two-phase flow in the vaneless gap between the runner blades and the guide vanes of the reduced scale model: when the power consumption is at its minimum, the air–water flow is not interacting with the runner. On the other side, when the air–water flow periodically interacts with the runner blades, the power consumption increases and so the resulting P_{nD} absolute value also increases and goes far beyond the absolute value of the P_{nD} of the prototype. Therefore, the power consumption during SC mode in the reduced scale model could be transposed to the full scale prototype, but the validation of this transposition requires further experiments including the full homology of the draining system on the reduced scale model tests, as it would be too dangerous to test the full-scale prototype with a closed draining pipe.

5. Conclusion

In the present study, the dynamic behaviour of a full-scale Francis turbine operating in synchronous condenser mode has been investigated by on-site experimental tests and reduced scale physical model experiments. The measurement of the draft tube wall vibrations allows for the detection of the sloshing motion of the water in the draft tube cone at the frequency close to the free-surface gravity wave natural frequency as also predicted by the experiments performed on the homologous reduced scale physical model [11], and observed in literature [10,18].

Measurements of the runner stresses, guide vanes vibrations and torque fluctuations highlight the benefits of draining completely the runner and the surrounding vaneless gap between the runner blades and the closed guide vanes by injecting pressurized air and by installing an efficient draining pipe to drain the water accumulating in the vaneless gap. Accordingly to Guillaume et al. [24], the evidence of the advantages of the draining pipe is confirmed on the full scale prototype by observing a low amplitude of the runner and guide vanes vibrations due to the rotor–stator interaction and a lack of further fluctuations correlated to the air–water mixing phenomena in the vaneless gap.

Furthermore, the average value of the consumed active power is reduced to 3% of the turbine rated power and no power oscillations are highlighted. It proves the importance of the runner draining to guarantee the absence of dangerous two-phase flow phenomena compromising the machine operation and the safety of both the mechanical and electrical components. This also confirms that the sloshing motion does not play a key role during the SC mode operation since it does not cause machine vibrations impacting on the power consumption, as also observed in the reduced scale model.

The results achieved in this paper allows for the understanding of the dynamic behaviour of a Francis turbine during SC mode to guarantee a safe operation of the hydroelectric unit while providing voltage regulation to the EPS. The performed analysis on the results of both the reduced scale model and the full scale prototype suggests the methodology to study the SC mode operation on the reduced scale model and a possible results transpositions to the full scale prototype. In particular, it is highlighted the importance of respecting the densimetric Froude number similarity and the necessity of controlling the two-phase flow phenomena due to the air–water mixing in the vaneless gap between the runner blades and the guide vanes by installing a draining pipe to guarantee the complete draining of the runner chamber. To validate the methodology of the power consumption transposition, the full homology of the draining system in the reduced scale model should be respected and, therefore, further investigations should be performed with this configuration.

CRediT authorship contribution statement

E. Vagnoni: Data curation, Conceptualization, Methodology, Investigation, Formal analysis, Validation, Visualization, Writing - original draft. **D. Valentin:** Data curation, Resources, Investigation, Writing - review & editing. **F. Avellan:** Writing - review & editing, Supervision, Project administration, Funding acquisition.

Declaration of Competing Interest

The authors declare that they have no known competing financial interests or personal relationships that could have appeared to influence the work reported in this paper.

Acknowledgments

The research leading to the results published in this paper is part of the HYPERBOLE Research Project, granted by the European Commission (ERC/FP7-ENERGY-2013-1-Grant 608532); The authors would like to thank BC Hydro (CA) for making available the prototype generating unit for tests. In particular thanks to Danny Burggraeve, Jacob Iosfin, and their staff. thanks also to Voith Hydro and GE Renewable Energy for the strain gauges and pressure sensors installation.

References

[1] European commission energy roadmap, 2050. doi:10.2833/10759.
[2] Jones D, Mansoor S, Aris F, Jones G, Bradley D, King D. A standard method for specifying the response of hydroelectric plant in frequency-control mode. Electric Power Syst Res 2004;68(1):19–32. https://doi.org/10.1016/S0378-7796(03)00152-4.
[3] Khodabakhshian A, Hooshmand R. A new pid controller design for automatic generation control of hydro power systems. Int J Electr Power Energy Syst 2010;32(5):375–82. https://doi.org/10.1016/j.ijepes.2009.11.006.
[4] Skok S, Ivankovic I, Zbunjak Z. Two layer hydropower plant dynamic mathematical modelling using synchronized measurements. Int J Electr Power Energy Syst 2018;103:302–9. https://doi.org/10.1016/j.ijepes.2018.05.008.
[5] Saarinen L, Norrlund P, Yang W, Lundin U. Linear synthetic inertia for improved frequency quality and reduced hydropower wear and tear. Int J Electr Power Energy Syst 2018;98:488–95. https://doi.org/10.1016/j.ijepes.2017.12.007.
[6] Rychkov IG. Reactive power control services based on a generator operating as a synchronous condenser. Power Technol Eng 2013;46:405–9.

[7] Rossi G, Zanetti V. Starting in air and synchronous condenser operation of pump-turbines - model research. Proceedings of the 9th IAHR-SHMEC Symposium, 2. USA: Fort Collins; 1978. p. 337–52.
[8] Magsaysay G, Schuette T, Fostiak RJ. Use of a static frequency converter for rapid load response in pumped-storage plants. IEEE Trans Energy Convers 1995;10(4):694–9.
[9] Giosio DR, Henderson AD, Walker JM, Brandner PA. Rapid reserve generation from a francis turbine for system frequency control. Energies 2017;10(4). https://doi.org/10.3390/en10040496.
[10] Tanaka H, Matsumoto K, Yamamoto K. Sloshing motion of the depressed water in the draft tube in dewatered operation of high head pump-turbines. Proceedings of the XVII IAHR Symposium on hydraulic machines and cavitation, Beijing, China, 1. 1994. p. 121–30.
[11] Vagnoni E, Favrel A, Andolfatto L, Avellan F. Experimental investigation of the sloshing motion of the water free-surface in the draft tube of a francis turbine operating in synchronous condenser mode. Exp Fluids 2018;59(6):95.
[12] Vagnoni E, Andolfatto L, Guillaume R, Leroy P, Avellan F. Rotating air-water ring in the vaneless gap of a pump-turbine operating in condenser mode. Int J Multiph Flow 2018;105:112–21. https://doi.org/10.1016/j.ijmultiphaseflow.2018.03.022.
[13] Vagnoni E, Andolfatto L, Guillaume R, Leroy P, Avellan F. Interaction of a rotating two-phase flow with the pressure and torque stability of a reversible pump-turbine operating in condenser mode. Int J Multiph Flow 2019;111:112–21. https://doi.org/10.1016/j.ijmultiphaseflow.2018.11.013.
[14] Vagnoni E, Andolfatto L, Guillaume R, Leroy P, Avellan F. Oxygen diffusion through air-water free surfaces in a pump-turbine operating in condenser mode. Int J Multiph Flow 2019;112:183–92. https://doi.org/10.1016/j.ijmultiphaseflow.2018.11.011.
[15] Snyder WH. Similarity criteria for the application of fluid models to the study of air pollution meteorology. Bound-Layer Meteorol 1972;3:113–34.
[16] Odell GM, Kovasznay LSG. A new type of water channel with density stratification. J Fluid Mech 1971;50(3):535–43. https://doi.org/10.1017/S002211207100274X.
[17] Valentine D, Frandsen J. Nonlinear free-surface and viscous-internal sloshing. J Offshore Mech Arct Eng 2005;127:141–9.
[18] Ceravola O, Fanelli M, Lazzaro B. The behaviour of the free level below the runner of francis turbine and pump-turbines in operation as synchronous condenser. Proceedings of the 10th IAHR-SHMEC Symposium, Tokyo, Japan 1980;1:765–75.
[19] Valentín D, Presas A, Valero C, Egusquiza M, Egusquiza E. Synchronous condenser operation in francis turbines: Effects in the runner stress and machine vibration. Renewable Energy 2020;146:890–900. https://doi.org/10.1016/j.renene.2019.07.041.
[20] Guillaume R, Lowys PY, egrand A, Girin P. Hydraulic installation operating in condenser mode, https://patentscope.wipo.int/search/en/detail.jsf?docId=WO2017046012, patent WO/2017/046012, IPC F03B 11/00 3/02 (2006.01); 2017.
[21] Egusquiza E, Valentín D, Presas A, Valero C. Overview of the experimental tests in prototype. J Phys: Conf Ser 2017;813:012037. https://doi.org/10.1088/1742-6596/813/1/012037.
[22] Gomes Pereira Junior J, Andolfatto L, Favrel A, Landry C, Nicolet C, Alligné S, et al. Procedure for predicting part load resonance in francis turbines hydropower units based on swirl number and local cavitation coefficient similitude. Mech Syst Signal Process 2019;132:84–101. https://doi.org/10.1016/j.ymssp.2019.06.011.
[23] Zobeiri A. Investigations of time dependent flow phenomena in a turbine and a pump-turbine of francis type: Rotor-stator interactions and precessing vortex rope, Ph.D. thesis, EPFL; 2009.
[24] Synchronous condenser systems, General Electric - Digital Energy.